Abstract #05614 ISMRM ABSTRACT

Uncertainty-Guided Active Learning for Access Route Segmentation and Planning in Transcatheter Aortic Valve Implantation

Primary: Cardiovascular - Vascular and Vessel Wall 〉 **Secondary:** Analysis Methods - Segmentation and Detection 〉 **Digital Poster** · 60 min | Congenital Heart Disease, Valves, and Vessels · Wednesday, May 13 at 01:40 PM 〉 **Keywords:** ACTIVE LEARNING VESSEL DIAMETER QUANTIFICATION AORTIC SEGMENTATION TAVI PLANNING CARDIOVASCULAR MAGNETIC RESONANCE

Enrique Almar-Munoz [1], **Mahdi Islam** [1], **Musarrat Tabassum** [1], **Christian Kremser** [1], **Markus Haltmeier** [2], **Agnes Mayr** [1]

[1]Medical University of Innsbruck, Innsbruck, Austria
[2]University of Innsbruck, Austria

Presenting Author: *Enrique Almar-Munoz (enrique.almar@i-med.ac.at)*

Impact

This work enables accurate, low-annotation CMR-based vascular assessment for TAVI, reducing dependence on CT and contrast agents while achieving precise vessel segmentation and diameter quantification through uncertainty-guided active learning, improving access route planning in patients with renal impairment.

Synopsis

Motivation: Transcatheter Aortic Valve Implantation (TAVI) requires accurate vascular access route assessment, but CTA's contrast agents pose risks for patients with renal impairment. CMR offers a safer alternative but demands extensive manual segmentation.

Goals: To develop an annotation-efficient CMR-based pipeline for aorto-iliac segmentation and access route quantification.

Approach: We implemented an uncertainty-guided active learning framework with pseudo-labelling for post-contrast CMR, integrated with automated centerline extraction and continuous diameter measurement.

Results: Experimental results demonstrated strong performance, achieving Dice scores of 0.966 for aorta and 0.844 for iliacs, with a mean absolute percentage error of 4.92% in diameter estimation.

Introduction

Transcatheter Aortic Valve Implantation (TAVI) is the standard treatment for severe aortic stenosis in patients unsuitable for open-heart surgery [1]. The selection of the optimal vascular access route is crucial to minimise complications. Computed Tomography Angiography (CTA) remains the reference imaging modality for TAVI planning [2], yet it relies on iodinated contrast agents that pose nephrotoxic risks to patients with chronic kidney disease. Cardiovascular Magnetic Resonance (CMR) provides an iodinated contrast-free alternative [3]. However, deep learning–based segmentation methods require large amounts of annotated data for training, making dataset creation expensive and time-consuming.

Active learning (AL) methods that iteratively select the most informative samples for expert annotation can significantly reduce labelling burden. This study presents an **uncertainty-guided active learning pipeline** for accurate segmentation and diameter quantification of the aorta and iliac arteries in post-contrast CMR, designed to support TAVI access route planning.

Dataset

An in-house dataset of 337 CMR scans was retrospectively analysed, including 166 pre-contrast and 171 post-contrast acquisitions from patients enrolled in the TAVR-CMR clinical trial conducted between Medical University of Innsbruck and Wels-Grieskirchen Hospital, between 2017–2022 [4,5]. Imaging was performed on a 1.5 T Siemens MAGNETOM AVANTOfit scanner using standardised whole-heart 3D SSFP and 3D FLASH MRA sequences before and after intravenous gadobutrol ($0.2mmol/kg$).

Methods

The full pipeline is shown in Figure 1.

1. Automated Vessel Diameter Quantification

1. **Centerline Extraction:** The binary vessel mask was skeletonized to obtain a 1-voxel-wide medial axis. The largest connected component was converted into a graph, and the longest shortest path between endpoints (via Dijkstra's algorithm [6]) defined the centerline.
2. **Refinement:** The centerline coordinates were smoothed using a uniform filter, and endpoints were corrected toward the vessel's center of mass for robustness.
3. **Diameter Estimation:** For each centerline point, local diameters were calculated using a hybrid approach combining a 3D Euclidean Distance Transform (EDT) [7] and a ray-casting method [8] across orthogonal planes. The EDT-derived and ray-based diameters were averaged, interpolated if necessary, and smoothed via a Savitzky–Golay filter to produce continuous diameter profiles along the aorto-iliac route.

2. Uncertainty-Guided Active Learning for Segmentation (depicted in Figure 2)

The segmentation backbone employed nnU-Net v2 with a Residual Encoder U-Net preset [9], trained with Dice + Cross-Entropy loss and PolyLR learning rate decay.

- The 171 post-contrast scans were divided into 145 training and 26 hold-out test cases.
- Initially, 15 scans were manually annotated.
- At each AL iteration, model-predicted probability maps were analyzed to compute case uncertainty scores combining voxel-wise entropy and the proportion of high-confidence voxels.
- The three most uncertain cases were manually annotated, while the twelve most certain were pseudo-labelled.
- Training, inference, and selection were repeated until performance plateaued.

3. Multimodal Ablation Study

After AL convergence, two architectures (3D U-Net [9] and UMamba [10]) were trained across four configurations. The Dice Similarity Coefficient (DSC) and Mean Absolute Percentage Error (MAPE) were computed for aorta and iliac segmentation and diameter estimation.

Results

Active Learning Performance

Performance improved substantially across AL iterations, plateauing after the fifth cycle (Figure 3). The mean Dice score increased from 0.789 to 0.912, while the iliac artery MAPE decreased from 18.4% to 8.3%. The most notable gains occurred in the first three iterations, confirming that uncertainty-driven sample selection accelerates learning and reduces annotation demand.

Segmentation and Diameter Accuracy

The best final model (3D U-Net trained on post-contrast CMR) achieved Dice scores of 0.966 ± 0.02 for the aorta and 0.844 ± 0.03 for the iliac arteries, with a MAPE of 4.92% in diameter estimation. Diameter profiles along the aorto-iliac path were physiologically consistent, ranging from $20–30mm$ proximally to $6–12mm$ distally, accurately reproducing the $5mm$ clinical threshold relevant for transfemoral access (Figure 4).

Ablation Study Findings

Post-contrast-only models consistently outperformed all multimodal configurations (Figure 5). Including inferred pseudo-labels from the unseen cases in the AL pipeline slightly degraded performance. Combining pre- and post-contrast inputs did not improve accuracy.

Discussion

This study demonstrates that uncertainty-guided active learning can substantially reduce manual annotation requirements while maintaining high segmentation accuracy in post-contrast CMR for TAVI planning. The hybrid uncertainty metric effectively identified informative samples, accelerating performance gains in early AL cycles and minimising labelling cost.

Clinically, replacing CTA with contrast-enhanced CMR in selected patients could eliminate nephrotoxic risk while providing accurate vessel measurements. The achieved Dice ($0.966/0.844$) and MAPE (4.9%) indicate that the method approaches expert-level accuracy, suitable for integration into semi-automated preoperative workflows where clinicians review model outputs guided by uncertainty maps.

Limitations include the single-center validation, dependence on post-contrast data, and error propagation from segmentation to diameter estimation.

Acknowledgements

This research was partially funded by the Austrian Science Fund (FWF), FWF DOC 110.

References

1. Díez, J. G. (2013). Transcatheter aortic valve implantation (TAVI): the hype and the hope. Texas Heart Institute Journal, 40(3), 298.

2. Al-Najafi, S., Sanchez, F., & Lerakis, S. (2016). The crucial role of cardiac imaging in transcatheter aortic valve replacement (TAVR): pre-and post-procedural assessment. Current treatment options in cardiovascular medicine, 18(12), 70. https://doi.org/10.1007/s11936-016-0497-z

3. Mahon, C., & Mohiaddin, R. H. (2021). The emerging applications of cardiovascular magnetic resonance imaging in transcatheter aortic valve implantation. Clinical Radiology, 76(1), 73-e21. https://doi.org/10.1016/j.crad.2019.11.011

4. Mayr, A., Klug, G., Reinstadler, S. J., Feistritzer, H. J., Reindl, M., Kremser, C., ... & Metzler, B. (2018). Is MRI equivalent to CT in the guidance of TAVR? A pilot study. European Radiology, 28(11), 4625-4634. https://doi.org/10.1007/s00330-018-5386-2

5. Reindl, M., Lechner, I., Holzknecht, M., Tiller, C., Fink, P., Oberhollenzer, F., ... & Reinstadler, S. J. (2023). Cardiac magnetic resonance imaging versus computed tomography to guide transcatheter aortic valve replacement: a randomized, open-label, noninferiority trial. Circulation, 148(16), 1220-1230. https://doi.org/10.1161/CIRCULATIONAHA.123.066498

6. Dijkstra, E. W. (2022). A note on two problems in connexion with graphs. In Edsger Wybe Dijkstra: his life, work, and legacy (pp. 287-290). https://doi.org/10.1145/3544585.3544600

7. Maurer, C. R., Qi, R., & Raghavan, V. (2003). A linear time algorithm for computing exact Euclidean distance transforms of binary images in arbitrary dimensions. IEEE Transactions on Pattern Analysis and Machine Intelligence, 25(2), 265-270. doi:10.1109/TPAMI.2003.1177156

8. Sato, Y., Nakajima, S., Atsumi, H., Koller, T., Gerig, G., Yoshida, S., & Kikinis, R. (1997, March). 3D multi-scale line filter for segmentation and visualization of curvilinear structures in medical images. In International Conference on Computer Vision, Virtual Reality, and Robotics in Medicine (pp. 213-222). Berlin, Heidelberg: Springer Berlin Heidelberg. https://doi.org/10.1007/BFb0029240

9. Isensee, F., Jaeger, P. F., Kohl, S. A., Petersen, J., & Maier-Hein, K. H. (2021). nnU-Net: a self-configuring method for deep learning-based biomedical image segmentation. Nature methods, 18(2), 203-211. https://doi.org/10.1038/s41592-020-01008-z

10. Ma, J., Li, F., & Wang, B. (2024). U-mamba: Enhancing long-range dependency for biomedical image segmentation. arXiv preprint arXiv:2401.04722.

Figures and Tables

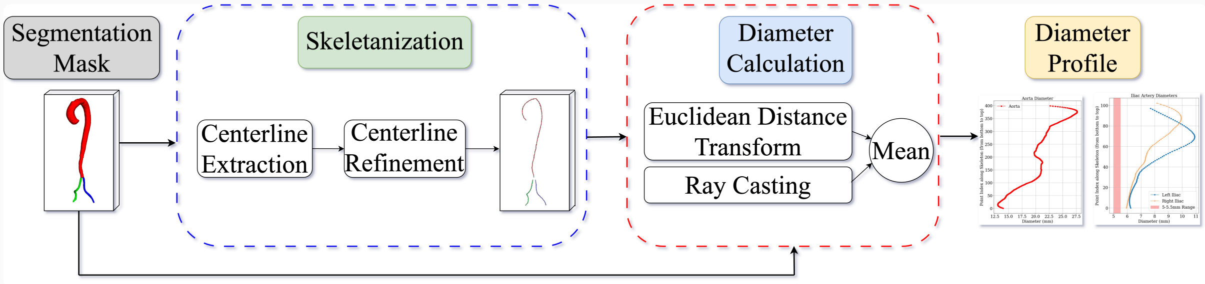

Scan for high-resolution version

Figure 1: *Overview of the automated vessel diameter quantification pipeline.*

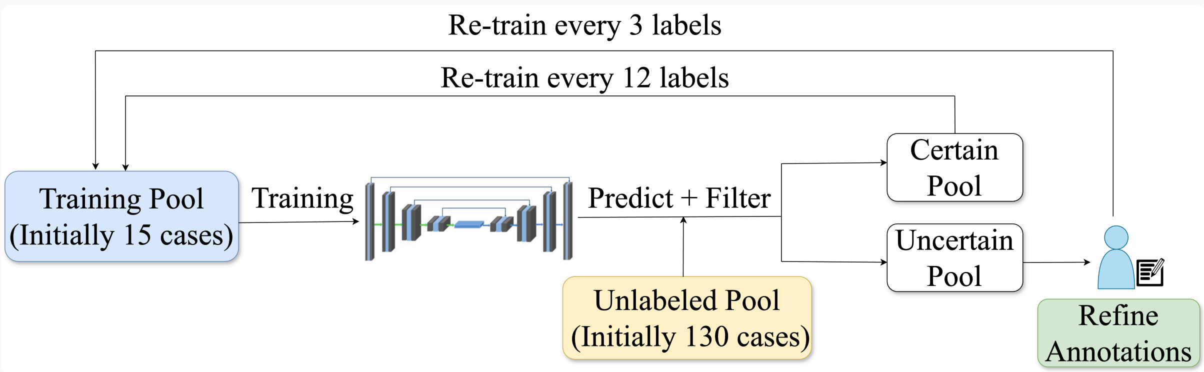

Scan for high-resolution version

Figure 2: *The active learning cycle includes training, inference on unlabelled data, uncertainty-based ranking, and sample selection, with uncertain cases manually annotated and certain ones pseudo-labelled to expand the training set.*

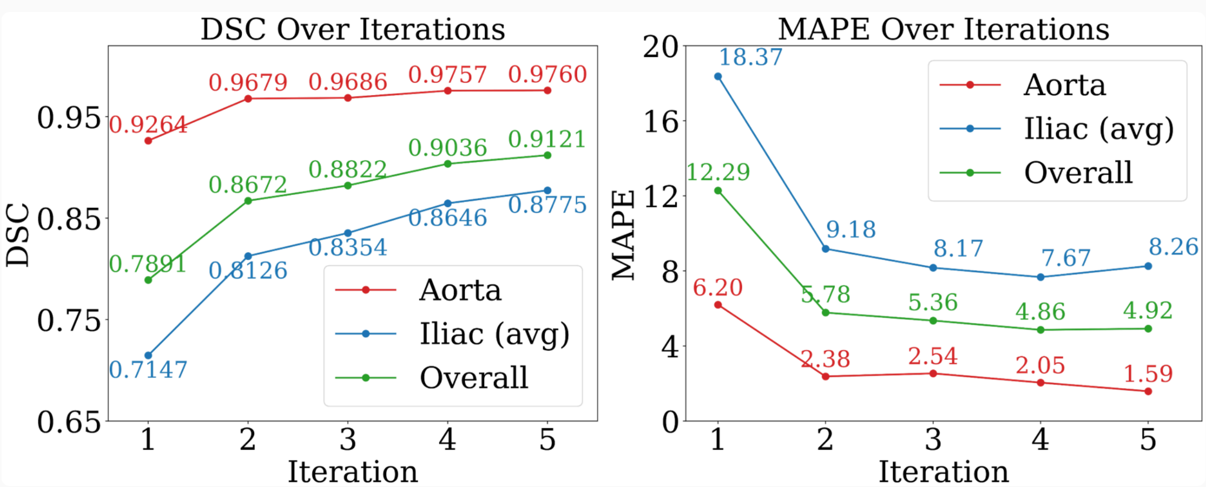

Scan for high-resolution version

Figure 3: *Performance of active learning across iterations for evaluation metrics. (left) Dice score; (right) mean absolute percentage error (MAPE).*

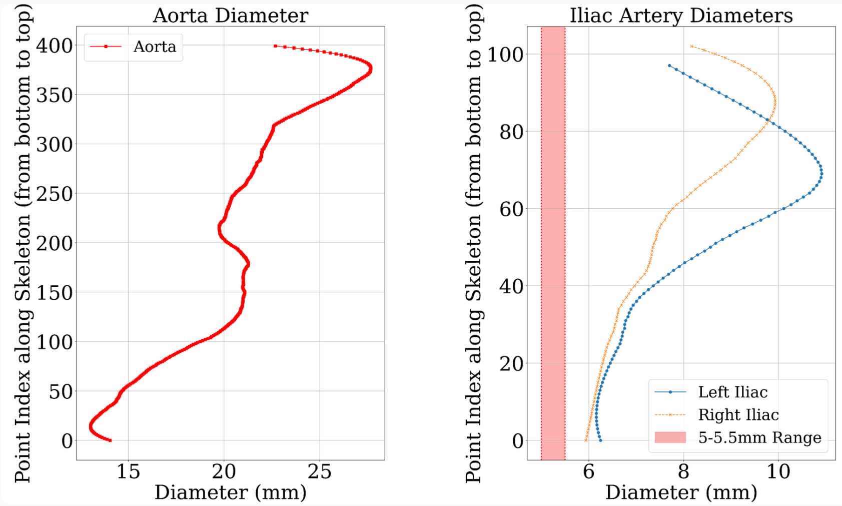

Scan for high-resolution version

Figure 4: *Diameter profiles of a representative sample. (left) The diameter measurements along the aorta. (right) The diameter measurements for the left and right iliac arteries, with the 5–5.5 mm reference threshold range indicated.*

Configuration	Model	Aorta	Left Iliac	Right Iliac	Average
Post	3D-UNet	0.9664	0.8250	**0.8627**	**0.8871**
	UMamba	0.9678	0.8111	0.8321	0.8732
Post + Inferred	3D-UNet	0.9626	0.8107	0.8507	0.8773
	UMamba	0.9617	**0.8272**	0.8260	0.8743
Pre&Post	3D-UNet	0.9667	0.8167	0.8132	0.8655
	UMamba	**0.9684**	0.8222	0.8404	0.8770
Pre&Post + Inferred	3D-UNet	0.9677	0.7991	0.7954	0.8541
	UMamba	0.9660	0.8152	0.7944	0.8585

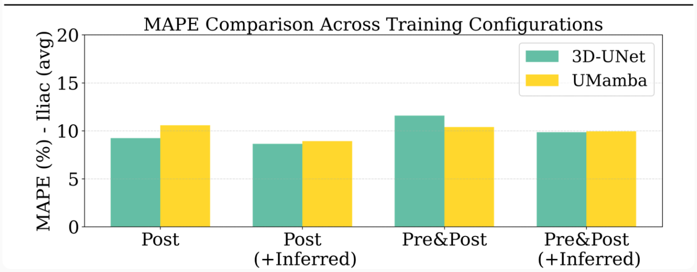

Scan for high-resolution version

Figure 5: *Ablation results for different training inputs: (top) Dice scores for aorta and iliac segmentation. For each metric, the single best result across all configurations is highlighted in bold. Results within 0.005 of the best score are underlined. Blue text indicates the pre-contrast dataset, while brown text marks configurations that include non-supervised inferred predictions. (bottom) MAPE scores for Iliac diameter across models and data configurations*